Covalent Binding and Interstrand Cross-Linking of Duplex DNA by Dirhodium(II,II) Carboxylate Compounds†

Shari U. Dunham,*,‡ Helen T. Chifotides,§ Szymon Mikulski,‡ Amity E. Burr,‡ and Kim R. Dunbar§

Department of Chemistry, Colby College, Waterville, Maine 04901, and Department of Chemistry, Texas A&M University, College Station, Texas 77843

Received June 26, 2004; Revised Manuscript Received October 27, 2004

ABSTRACT: The study of the interactions of double-stranded (ds) DNA with the dirhodium carboxylate compounds $Rh_2(O_2CCH_3)_4(H_2O)_2$ (Rh1), $[Rh_2(O_2CCH_3)_2(CH_3CN)_6](BF_4)_2$ (Rh2), and $Rh_2(O_2CCF_3)_4$ (Rh3) supports the presence of covalently linked DNA adducts, including stable DNA interstrand cross-links. The present biochemical study refutes earlier claims that no reaction between dirhodium compounds and dsDNA occurs. The reversal behavior of these interstrand cross-links in 5 M urea at 95 °C (for different heating times) implies the presence of various coordination modes involving *ax*/*ax*, *ax*/*eq*, and *eq*/*eq* DNA interactions with the dirhodium core. The reaction rates of the dirhodium compounds with dsDNA were determined spectroscopically and are in the order Rh1 ≪ Rh2 < Rh3. This difference in behavior of the three dirhodium compounds correlates with the lability of the leaving groups and corresponds to the extent of interstrand cross-link formation by these compounds on a 123 bp DNA fragment, as observed by denaturing polyacrylamide gel electrophoresis (dPAGE). Since all three dirhodium compounds form covalent Rh−DNA adducts, including interstrand cross-links, it is important that DNA be considered a potential target for biological activity of these dirhodium carboxylate compounds.

Metal-based antitumor drugs have the ability to target DNA by forming various covalent adducts. The resounding success of *cis*-$Pt(NH_3)_2Cl_2$ (*cis*-DDP or cisplatin)[1] as a prominent chemotherapeutic agent stems from the covalent cross-links formed with DNA (*1*−*3*) which inhibit transcription and DNA replication (*4*−*7*). These Pt−DNA covalent cross-links, which occur at N7 of guanine or adenine bases, include bifunctional intrastrand (∼65% GG, ∼25% AG) and interstrand adducts (∼6% at 5′-GC-3′ and 5′-CG-3′), as well as minor amounts of monofunctional and 1,3-intrastrand adducts (*8*, *9*). Although the intrastrand adducts are the most abundant and are believed to be responsible for *cis*-DDP antitumor activity (*1*), it is possible that a small number of highly toxic interstrand cross-links are important for *cis*-DDP biological activity (*9*, *10*). In addition, interstrand lesions lead to a unique profile of antitumor activity for dinuclear and trinuclear platinum compounds that are considerably different DNA-modifying anticancer agents from *cis*-DDP (*11*, *12*).

Despite the efficacy of *cis*-DDP (*1*), its limitations (*9*) have led to the screening of other metal-based compounds for antitumor activity. Among the promising non-platinum antitumor complexes (*13*) are dirhodium compounds of the type $Rh_2(O_2CR)_4L_2$ (R = Me, Et, Pr; L = solvent) that contain at least two bridging carboxylate ligands (Figure 1) (*14*). Pioneering studies in the 1970s revealed that dirhodium carboxylate compounds exhibit significant in vivo antitumor activity against L1210 tumors (*15*, *16*), Ehrlich ascites (*17*−*23*), sarcoma 180, and P388 tumor lines (*24*). Although the exact mechanism of their antitumor activity has not been elucidated (*25*), plausible cellular targets that have been reported are single-stranded (ss) DNA (*17*, *18*, *24*), polymerases (*26*, *27*), and other proteins (*28*−*33*).

Early studies aimed at understanding the interactions of dirhodium compounds with DNA led to the conclusion that reactions occurred only with poly(A) and not with double-stranded (ds) DNA, poly(G), or poly(C) (*18*, *24*, *29*, *34*, *35*). In these initial studies (*18*, *29*), the ^{14}C-labeled acetate ligand rather than Rh metal was monitored in dirhodium compound−DNA reactions by dialysis experiments. In the latter study (*34*), melting curves and sedimentation data of calf thymus DNA changed only at extremely high dirhodium compound concentrations and long reaction times. Subsequent reactions between model nucleobases and dirhodium compounds indicate a strong preference for axial (*ax*) binding of adenine (via the purine atoms N7 or N7/N1) (*36*−*42*) as compared

† This work was supported by the Howard Hughes Medical Institute (institutional grant to Colby College), a grant from the Colby College Natural Sciences Division (to S.U.D.), the Colby College Student Special Project Funds (to A.E.B.), and grants to K.R.D. from the Welch Foundation (A-1449) and the National Science Foundation (CHE-9906583).

* To whom correspondence should be addressed. Tel: 207-859-5762. Fax: 207-872-3804. E-mail: sudunham@colby.edu.

‡ Colby College.

§ Texas A&M University.

[1] Abbreviations: *cis*-DDP or cisplatin, *cis*-diamminedichloroplatinum(II); ss, single stranded; ds, double stranded; 9-EtGua, 9-ethylguanine; 5′-GMP, guanosine 5′-monophosphate; Rh1, $Rh_2(O_2CCH_3)_4(H_2O)_2$; Rh2, $[Rh_2(O_2CCH_3)_2(CH_3CN)_6](BF_4)_2$; Rh3, $Rh_2(O_2CCF_3)_4$; bp, base pairs; ax, axial; eq, equatorial; GFAAS, graphite furnace atomic absorption spectroscopy; PAGE, polyacrylamide gel electrophoresis; dPAGE, denaturing polyacrylamide gel electrophoresis; 1×TBE buffer, 90 mM tris(hydroxymethyl)aminomethane, 90 mM boric acid, and 2 mM EDTA, pH 8.0; R_b, bound ratio or moles of bound metal compound per mole of DNA base pairs; R_f, formal ratio or moles of reacted metal compound per mole of DNA base pairs; *trans*-DDP, *trans*-diamminedichloroplatinum(II); CT-DNA, calf thymus DNA; NaOAc, sodium acetate.

10.1021/bi0486637 CCC: $30.25 © 2005 American Chemical Society
Published on Web 12/30/2004

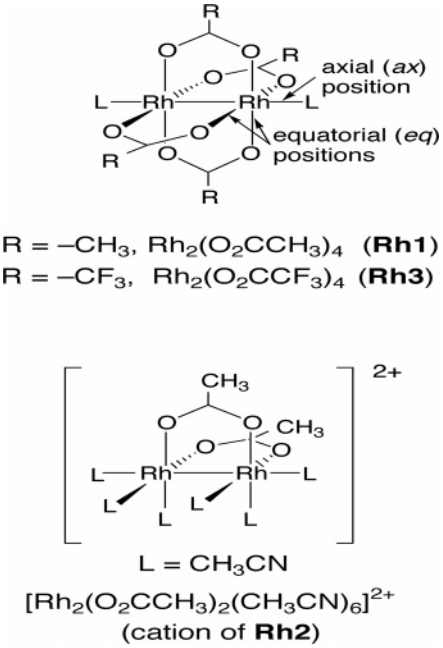

FIGURE 1: Dirhodium(II,II) carboxylate compounds included in this study.

to guanine. Crystal structural determinations, however, of dirhodium complexes with 9-ethylguanine (9-EtGua) revealed unprecedented bridging 9-EtGua groups at equatorial (*eq*) positions of the dirhodium unit via the N7/O6 purine sites (*43*, *44*). One- and two-dimensional NMR studies of $Rh_2(O_2CCH_3)_4$ reactions with guanosine 5′-monophosphate (5′-GMP) and the dinucleotides d(GpG) and d(pGpG) support similar binding modes with the guanine rings occupying eq positions via N7/O6 (*45*, *46*). In addition, mass spectrometry and enzymatic digestion studies of dirhodium adducts with ssDNA oligonucleotides corroborate binding of the purine bases (*47*, *48*).

Herein, we report an investigation of the interactions of dsDNA with dirhodium carboxylate compounds by biochemical methods, the results of which unequivocally support the presence of covalently linked Rh−DNA adducts, including stable Rh−DNA interstrand cross-links. This study of dirhodium−dsDNA adducts, which correlates the structure of the dirhodium compounds with the kinetics of adduct formation, refutes earlier claims that no reaction between dirhodium compounds and dsDNA occurs. The nature of these adducts along the duplex has been addressed. The importance of these adducts is critical to understanding the biological activity of these potential antitumor agents.

MATERIALS AND METHODS

Metal Compounds. The dirhodium compounds $Rh_2(O_2CCH_3)_4(H_2O)_2$ = Rh1 (*49*), $[Rh_2(O_2CCH_3)_2(CH_3CN)_6](BF_4)_2$ = Rh2 (*50*), and $Rh_2(O_2CCF_3)_4$ = Rh3 (*51*, *52*) (Figure 1) were prepared according to literature procedures. The *cis* and *trans* isomers of $Pt(NH_3)_2Cl_2$ were purchased from Alfa Aesar and Acros Chemicals, respectively.

Nucleic Acids. Salmon testes DNA (type III, D1626) was purchased from Sigma in powder form. The DNA pellet was dissolved in 1.5 mM phosphate buffer and 15 mM NaCl at pH 6.0 and filtered through a 0.45 μm filter before use. DNA purity and concentration (moles of base pairs per liter) were determined by UV absorption measurements at 230, 260, and 280 nm (∼660 g/mol of DNA base pairs) (*53*).

A 123 bp DNA fragment of known sequence (Figure S1) (*54*) was prepared as previously described (*55*) by an *Ava*I restriction digest of the 123 bp DNA ladder (Invitrogen) followed by purification on an 8% native polyacrylamide gel. The resulting purified fragment was radiolabeled with either a fill-in reaction (using [α-^{32}P]dCTP, [α-^{32}P]dTTP, or [α-^{32}P]dATP and the exo$^-$ mutant of the Klenow fragment of DNA polymerase I) or an end-labeling reaction (using [γ-^{32}P]ATP and T4 polynucleotide kinase). Following end-labeling with [γ-^{32}P]ATP, the 123 bp DNA was used to generate radiolabeled 86 bp and 41 bp DNA fragments by *Hae*III restriction enzyme digestion followed by purification on a 12% native polyacrylamide gel.

A 278 bp DNA fragment of known sequence was prepared from the *Eco*RI/*Bsu*36I restriction digest of M13mp18 plasmid DNA (New England Biolabs). The digestion products were radiolabeled with [α-^{32}P]dATP using the exo$^-$ mutant of the Klenow fragment of DNA polymerase I. Following labeling, the 278 bp fragment was purified on a 5% native polyacrylamide gel.

All DNA modification enzymes were purchased from New England Biolabs, and all radionucleotides were purchased from Amersham Biosciences.

Metal−DNA Reactions. DNA modification reactions with dirhodium and platinum compounds were carried out at 200 μM DNA base pairs (salmon testes DNA) and metal compound concentrations ranging from 0 to 20 μM in 1 mM phosphate buffer and 3 mM NaCl at a pH of 6.9 at 37 °C in the dark. Reactions with radiolabeled DNA fragments also included ∼10^5 cpm of labeled duplex along with the carrier salmon testes DNA. Fresh stock solutions (∼1 mM) of each metal compound were prepared in deionized water, diluted, and immediately used for DNA modification reactions.

For nonradioactive reactions, aliquots were sampled at specific times, immediately diluted 10-fold with 0.2 M NaCl to minimize electrostatic interactions of potentially solvated cationic dirhodium species with DNA, and concentrated by centrifugal filtration (Millipore Ultrafree devices, 30K MWCO). The concentrated aliquots were diluted at least 10-fold with deionized water followed by centrifugal filtration in the same devices, rinsed, and centrifuged repeatedly until the buffer and unreacted dirhodium compounds were completely removed (as determined from rhodium compound only controls). Reaction point time aliquots were analyzed for DNA concentration by UV−vis spectrophotometry and for bound rhodium concentration by using a Thermo Jarrell Ash-Smith Hieftje 22 atomic absorption spectrometer with a graphite furnace analyzer (GFAAS). Rhodium metal was measured at 343 nm with linear response over the range of 30−1200 ppb.

Polyacrylamide Gel Electrophoresis (PAGE) of Metal−DNA Reactions. To identify the presence of stable DNA interstrand cross-links, aliquots of metal−DNA reactions were made 5 M in urea, heated for 0−30 min at 95 °C, and then analyzed directly by 5% denaturing PAGE (dPAGE). Gels were prerun for 1−2 h at 300 V in 1×TBE buffer, electrophoresed at 300 V for 1−2 h, dried under vacuum, and then autoradiographed following film exposure at −20 °C. Intensities of DNA bands in gels were quantitated by

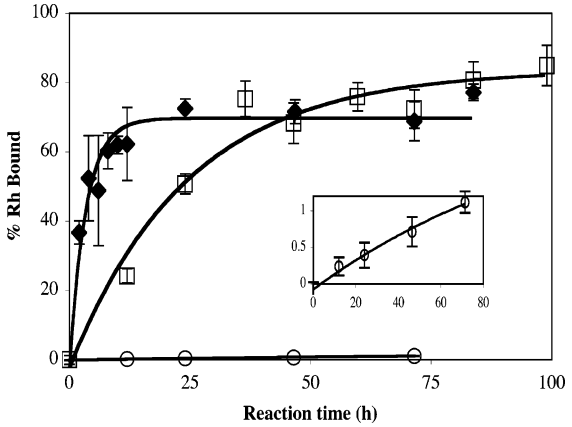

FIGURE 2: Rhodium−DNA-binding curves determined by UV−vis (for [DNA]) and GFAAS (for [Rh]) for reactions between Rh1 at 20 μM (○), Rh2 at 2 μM (□), or Rh3 at 400 nM (◆) and salmon testes duplex DNA (200 μM DNA bp). Values on the *y*-axis (% Rh bound = $R_b/R_f \times 100$) represent the percentage of initial rhodium compound that is bound to DNA after a given reaction time. Reaction conditions: 37 °C in the dark in 1 mM sodium phosphate buffer at pH 7.0 with 3 mM sodium chloride at rhodium compound/DNA bp ratios (R_f values) of 0.1 for Rh1, 0.01 for Rh2, and 0.002 for Rh3. Error bars represent one standard deviation from triplicate measurements. The inset graph is the expanded curve for the Rh1 data. All data are fit to exponential buildup of product in a first-order reaction.

Table 1: Initial Rates for the Reactions between Each Dirhodium Compound and dsDNA

compound	R_f	initial rate[a] (nM/h)	±error[c] (nM/h)
Rh1	0.1	2.4	0.2
Rh2	0.01	35.9	0.6
Rh3	0.002	57	15
Rh3	0.01[b]	1190	335

[a] Determined from the initial slope of the binding curves shown in Figure 2. [b] Binding curve not shown in Figure 2. [c] Uncertainty expressed as one standard deviation.

phosphorimagery on a Bio-Rad GS-505 molecular imaging system using Molecular Analyst software version 2.1.2.

When radiolabeled DNA samples were purified by native PAGE (DNA duplexes) or dPAGE (interstrand cross-linked DNA), the gels were not dried but exposed while wet to film at 4 °C. Using the developed film as a template, the desired radiolabeled bands were excised, and the DNA was eluted from the gel slice using the crush-and-soak method (*56*) at room temperature with vigorous shaking over several hours. The supernatants from these elutions were filtered (0.2 μm) and subsequently ethanol-precipitated to desalt and concentrate the DNA.

RESULTS

DNA-Binding Curves. The DNA-binding curves of the three dirhodium compounds (Rh1, Rh2, and Rh3**)** over time are compared in Figure 2. Reaction time point aliquots were processed by centrifiltration to remove unbound rhodium and then analyzed to determine R_b (the molar ratio of bound rhodium to DNA base pairs). In each reaction, the starting solution was directly analyzed to determine R_f (the molar ratio of total rhodium compound to DNA base pairs in the original reaction). As shown in Figure 2, the percent of DNA-bound rhodium (which is equal to $R_b/R_f \times 100$) increases

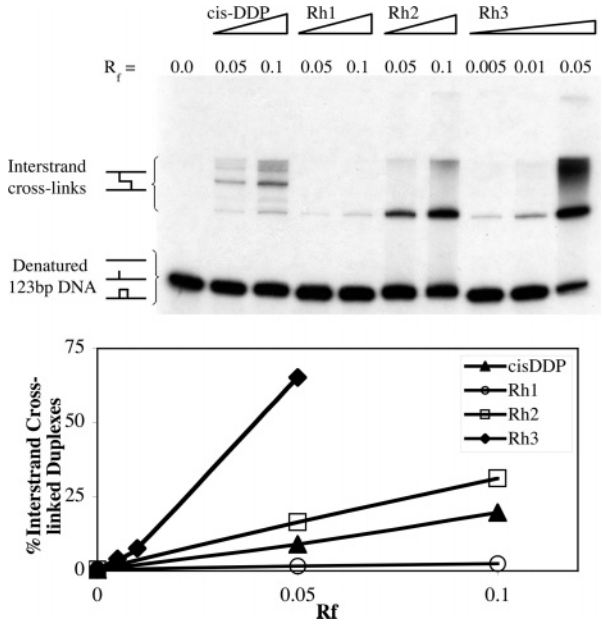

FIGURE 3: Denaturing PAGE (5%) of reactions between *cis*-DDP, Rh1, Rh2, or Rh3 and radiolabeled 123 bp DNA duplex (upper panel). Reactions were run for 23 h at conditions identical to those in Figure 2 with the addition of ~10^5 cpm of radiolabeled duplex and metal compound/DNA bp ratios (R_f values) as indicated at the top of each lane. The relative band intensities of the interstrand cross-links in the gel (upper panel) were determined by phosphorimagery and plotted vs R_f for each metal compound (lower panel).

over time for the three dirhodium compounds. Rh3 reacts most rapidly, even at very low metal concentrations ($R_f \sim$ 0.2 Rh/100 bp), and achieves complete binding after approximately 10 h. Rh2 requires greater initial concentrations ($R_f \sim$ 1 Rh/100 bp) to achieve maximum binding after 2 days; for comparison, Rh3 achieves the same maximum binding (~80%) within 2 h of reaction at the same initial dirhodium concentration of 2 μM ($R_f = 0.01$; data not shown). In contrast, even at very high dirhodium concentrations ($R_f \sim$ 10 Rh/100 bp), only ~1% of Rh1 binds covalently to DNA ($R_b \sim$ 1 Rh/1000 bp) after several days under the same reaction conditions. Due to slow reactivity, DNA reactions with Rh1 were not monitored over a long enough period of time to observe a binding plateau.

The DNA-binding curve data were fit to the exponential buildup of product in a first-order reaction (Figure 2). Initial reaction rates (Table 1) were determined from a linear fit of initial buildup of R_b vs time of data from the same reactions. These preliminary kinetic data rank reactivity of the dirhodium compounds with duplex DNA in the order Rh3 > Rh2 ≫ Rh1.

DNA Interstrand Cross-Linking. Compared to the high mobility band of denatured 123 bp DNA running at the bottom of the denaturing gel in Figure 3 (upper panel), bands of significantly lower mobility are observed in the DNA duplex reactions with metal compounds after 23 h. These lower mobility bands most likely result from DNA interstrand adducts (DNA that has been covalently cross-linked between the two strands of the duplex) (*57*). The aforementioned assignment is confirmed by the observation that, in a denaturing gel, these lower mobility bands run just slightly faster than a denatured 278 base fragment (Figure S2) that is approximately twice their single-stranded length. Quantification by phosphorimagery indicates an increase in the

intensity of the cross-linked DNA bands (Figure 3, lower panel), which corresponds to an increase in the initial reaction concentration (R_f) of each metal compound. The amount of cross-linked DNA formed depends on the initial metal concentration (R_f), is largest for Rh3, decreases in the order Rh3 > Rh2 > *cis*-DDP > Rh1, and is supported by the kinetic data from the DNA-binding curves (Figure 2).

Although *cis*-DDP is reported to form only small amounts (~6%) of interstrand cross-links on duplex DNA (*9*), it appears to form more than one type/position of interstrand cross-link on this 123 bp DNA fragment, as indicated by the multiple resolved lower mobility bands observed most clearly in lane 3 ($R_f = 0.1$, ~12 Pt/duplex) of the denaturing gel (Figure 3, upper panel). Similar dPAGE analyses of reactions between *trans*-DDP and 123 bp DNA have been performed (Figure S3) and also result in multiple resolved lower mobility bands in the region of interstrand cross-links (*58*). DNA bands of retarded mobility (interstrand cross-links) are also observed in the dPAGE of reactions between the 123 bp duplex and each of the three dirhodium compounds in this study (Figure 3). Unlike the platinum compounds, however, each dirhodium compound reacts with the DNA duplex to afford a major discrete band of shifted mobility (most clearly observed in lanes 5, 6, and 9 of Figure 3). Some lower mobility smearing is also observed and may be attributed to multiple dirhodium adducts on a single duplex due to the high R_f values (R_f > 1 Rh/123 bp). In addition, the same mobility major DNA band is observed for reactions of each dirhodium compound with the 123 bp fragment, regardless of the state of the ends of the DNA duplex: this same new band is observed by dPAGE of reactions of 123 bp DNA with dirhodium compounds when the DNA fragment has been radiolabeled with a fill-in reaction to form a blunt-ended duplex (data not shown) or 5′-end-labeled duplex to retain the 5′ overhangs of the restriction fragment.

Isolation and Stability Studies of the Interstrand Cross-Link. The major shifted band (interstrand cross-linked DNA) formed upon 123 bp DNA incubation with either Rh2 or Rh3 was isolated from a denaturing gel. The isolated DNA cross-links resulting from reaction with Rh2 (Figures 4 and S4) or Rh3 (Figure S4) were analyzed by dPAGE to determine the stability of the adducts to the isolation protocol. Under the sample preparation conditions that denature unmodified DNA in the absence of heat (Figure 4, lane 1), the major portion (~90%) of the isolated Rh2−DNA band still runs as the interstrand adduct (Figure 4, lane 2) as does almost all (~94%) of the isolated Rh3−DNA band (Figure S4, lane 1). Heating of the isolated cross-links, however, in 5 M urea at 95 °C for 5 min (Figure 4, lane 3), 15 min (Figure S4, lane 4), or 30 min (Figure S4, lanes 2 and 5) leads to approximately 30% reversal of each adduct. In Figure 4, additional conditions were explored to determine the stability of the interstrand Rh2−DNA cross-link; these include heating at 95 °C for 5 min in 40 mM thiourea (lane 4), 400 mM sodium acetate (lane 5), or 400 mM sodium carbonate (lane 6). For all of the tested conditions, the greatest degree of interstrand cross-link reversal (~70%) was achieved by heating the isolated Rh2 adduct in 40 mM thiourea prior to heating at 95 °C for 5 min in the urea-containing loading buffer (lane 4).

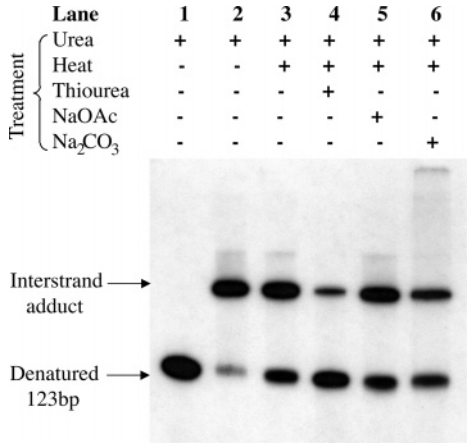

FIGURE 4: Denaturing PAGE (5%) of the isolated Rh2−interstrand cross-link formed on a 123 bp DNA duplex. Lane 1 contains unmodified 123 bp DNA. Lanes 2−6 contain the isolated cross-link followed by treatment with urea (5 M), heat (95 °C for 5 min), thiourea (40 mM), sodium acetate (400 mM), or sodium carbonate (400 mM), as indicated by the (+) signs above each lane.

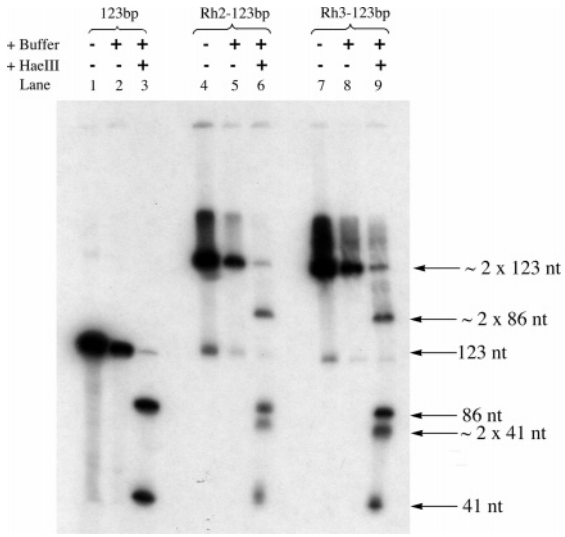

FIGURE 5: Denaturing PAGE (5%) of a 5′-end-labeled 123 bp DNA fragment reacted with dirhodium compounds before *Hae*III restriction endonuclease digestion. Lanes 1−3 contain unmodified 123 bp DNA, lanes 4−6 contain the isolated Rh2−123 bp interstrand cross-link, and lanes 7−9 contain the isolated Rh3−123 bp interstrand cross-linked DNA.

Isolated interstrand cross-links of Rh2 or Rh3 on the 123 bp DNA duplex were further analyzed by dPAGE following digestion with *Hae*III restriction endonuclease (Figure 5). Since the 123 bp sequence has a single *Hae*III site, cleavage of the unmodified 5′-end-labeled duplex at this site results in two radiolabeled fragments of 86 and 41 nucleotide lengths (lane 3). *Hae*III digestion of the isolated Rh2−123 bp interstrand cross-linked DNA (lane 6) results in a small amount of uncleaved adduct (at the mobility of ~2 × 123 nt) as well as four shorter fragments with greater mobility. The digestion results for the Rh3−123 bp interstrand cross-linked DNA (lane 9) are identical to those for Rh2 (lane 6).

DISCUSSION

Double-Stranded DNA Is a Viable Biological Target of Rhodium Compounds. The DNA-binding curves in this study (Figure 2) clearly indicate that the three dirhodium compounds under investigation bind covalently to dsDNA. The

relative reaction rates of these three dirhodium compounds with dsDNA (Rh3 > Rh2 ≫ Rh1; Table 1) corroborate those observed by mass spectrometry for ssDNA reactions (*48*). The increased DNA reactivity of Rh3 as compared to Rh1 also correlates with skin cell toxicity studies that indicate increased cytotoxicity of dirhodium compounds upon substitution of acetate with trifluoroacetate ligands (C. Turro, K. R. Dunbar, and co-workers, unpublished experiments).

Under the conditions of this study, Rh1 binds to dsDNA very slowly (Table 1), even at high R_f values. Although earlier studies concluded that Rh1 does not bind to dsDNA (*17*, *18*), these experiments monitored the amount of ^{14}C-labeled acetate ligands associated with dsDNA and not the Rh center(s) of the compounds directly (as the presently used method does). Subsequent reports clearly indicate that acetate ligand loss occurs in vivo (*59*), and therefore acetate ions are not a reliable probe for dirhodium binding (*43*−*46*, *48*, *60*). This is further supported by the fact that the reactions of Rh1 with 9-EtGua (*43*), 5′-GMP (*46*), d(GpG) (*45*), or d(pGpG) (*46*) proceed by substitution of two *cis*-acetate groups by the incoming nucleobase as well as protonation of the substituted acetate as monitored by ^{1}H NMR spectroscopy. Extensive loss of acetate groups has also been observed in the reactions of DNA octamer and dodecamer oligonucleotides with dirhodium carboxylate compounds (to the point of complete loss of all four carboxylate groups in the reactions of the latter), as monitored by mass spectrometry (*48*). Acetate ion loss most likely takes place concomitantly [the acetate group can be monodentate before being totally substituted by the incoming ligand (*61*)] with the nucleophilic attack of biological targets on the dirhodium species. In addition, the quantitative data of the present study are consistent with reported thermal denaturation data (*34*) which indicate changes in the melting profiles of CT-DNA upon reaction with Rh1 at extremely high R_f values and long reaction times.

The more rapid and efficient binding of Rh2 to dsDNA (Table 1**)**, which is significantly faster at one-tenth the dirhodium concentration of Rh1, may be attributed to the presence of monodentate CH_3CN groups in the eq positions of Rh2 instead of bridging acetate groups. This difference in reaction rates supports *eq* ligand loss as a required step to precede dirhodium *eq* interactions with DNA.

In the case of the trifluoroacetate analogue (Rh3), maximum binding to dsDNA is achieved in less than 10 h at extremely low R_f values (Figure 2). This enhanced reactivity relative to Rh2 at the same R_f (Table 1) may be attributed to the strong electron-withdrawing (inductive) effect of the CF_3 groups which renders the trifluoroacetate anion ($pK_b = 13.46$) a better leaving group than acetate ($pK_b = 9.25$) (*62*). This argument is further supported by the fact that the reaction of dirhodium tetrakis(trifluoroacetate) with 9-EtGua takes place without deprotonation of position N1 of the base, in contrast to the reaction of dirhodium tetraacetate (*43*). As has been shown by mass spectrometry, all four trifluoroacetate groups of Rh3 are substituted, even in reactions with short ss oligonucleotides (*48*).

Stable DNA Interstrand Cross-Links Are Formed by the Dirhodium Compounds. Denaturing gel analyses in this work indicate that, similarly to *cis*-DDP, interaction of dsDNA with dirhodium carboxylates leads to covalent cross-linking of the two strands of duplex DNA. Such interstrand cross-links were proposed in early structural studies of dirhodium carboxylate−tRNA adducts (*42*). The extent of DNA interstrand cross-link formation (Rh3 > Rh2 ≫ Rh1; Figure 3) correlates with the dirhodium compound DNA-binding rates determined in the present study (Table 1) and depends on the initial concentration of dirhodium compound in the DNA modification reactions (Figure 3, lower panel). The dPAGE gel in Figure 3 (upper panel) also indicates that Rh2 and Rh3 form a higher percentage of interstrand cross-links as compared to *cis*-DDP on this DNA duplex. Although the more abundant intrastrand DNA adducts of *cis*-DDP have been correlated with the drug efficacy (*1*) and have therefore been the focus of many antitumor studies of *cis*-DDP, the contribution to antitumor activity of a small amount of highly toxic adducts (such as interstrand cross-links) is still controversial (*9*, *10*). Therefore, it is possible that the interstrand cross-links formed by the dirhodium carboxylate compounds play an important role in their biological activity.

Previous studies of other DNA damaging agents have correlated the denaturing gel mobility of the DNA interstrand cross-link with the position of the cross-linked site relative to the ends of the DNA duplex (*8*). Specifically, covalent adducts that connect the two DNA strands closer to the end of the duplex have higher mobility (travel faster on a denaturing gel) than covalent adducts that bind to the DNA fragments closer to the center of the duplex. Considering the DNA sequence preferences for formation of interstrand cross-links by *cis*- and *trans*-DDP (*9*, *63*), it is not surprising that several resolvable bands of interstrand cross-linked DNA are observed from the reactions of the 123 bp DNA with *cis*-DDP (Figure 3) or *trans*-DDP (Figure S3). The fact that the pattern of intensity and mobility of these interstrand cross-linked bands is not the same for the 123 bp DNA modified with *trans*-DDP and *cis*-DDP lends further evidence that the bands represent different positioning of interstrand cross-links on this duplex (*8*).

Each of the three dirhodium compounds in this study form a major discrete band of interstrand cross-linked 123 bp DNA that has the same mobility in the denaturing gel as the highest mobility interstrand cross-link formed by *cis*-DDP (Figure 3). Although, within the resolution of dPAGE, this appears to be a single shifted band, it seems more likely that it does not represent a single interstrand cross-linked species. Rather, it is more likely a mixture of adducts cross-linked at similar positions relative to the end of the duplex but with different coordination modes including a mixture of monofunctional or bifunctional dirhodium adducts possibly bound at *ax*/*ax*, *ax*/*eq*, or *eq*/*eq* sites. This heterogeneity is supported by the interstrand cross-link behavior toward reversal conditions which indicates different chemical stability of the adducts (Figures 4 and S4). In Figure 4, lane 2 indicates that the interstrand adducts formed and isolated are stable to the conditions that denature unmodified DNA, although urea has been reported to form *ax* adducts with dirhodium tetraacetate by coordinating through the O of the carbonyl group (*64*). The stability of these *ax* adducts to the presence of urea in the absence of heat most likely is a kinetic issue enhanced by the inaccessibility of the dirhodium core due to steric hindrance of the DNA strands. The partial reversal (∼30%) of a subset of cross-links in 5 M urea by heating at 95 °C, regardless of the heating time (5, 15, or 30 min; Figures 4 and S4), suggests that the less stable adducts in the isolated

band are most likely *ax* DNA adducts which are expected to exhibit enhanced exchange rates upon heating as compared to *eq* DNA adducts (*65*). This argument is supported by the fact that, for $[Rh_2(eq\text{-}H_2O)_8(ax\text{-}H_2O)_2]^{4+}$, the rate of exchange of the *ax* H_2O molecules is 3 orders of magnitude higher than those in *eq* positions (*65*). Moreover, the Rh−N distances to an *eq* and *ax* CH_3CN molecule in *cis*-$[Rh_2(O_2CCH_3)_2(NCCH_3)_6](BF_4)_2$ of 1.985(4) and 2.232(4) Å, respectively (*50*), indicate that, for the same ligand, *ax* are weaker than *eq* interactions. Further heating in 40 mM thiourea induces reversal of additional adducts in the isolated band (up to ~70%), suggesting that another subset of adducts (most likely *eq* DNA adducts) is stable to more harsh reversal conditions. Substitution of the dirhodium core ligands in *eq* positions by thiourea (*66*) or other thiols (*67*, *68*) has precedent in the literature.

In addition, more than two fragments are observed by dPAGE (Figure 5, lanes 6 and 9) when these isolated bands of Rh2- or Rh3-modified 123 bp DNA are digested with *Hae*III (a restriction endonuclease with only a single recognition site in this sequence). The four new bands observed by dPAGE of digestions correspond to 5′-labeled 86 and 41 base fragments (observed in the digestion of unmodified DNA, lane 3), as well as fragments twice their size (expected for DNA that has an interstrand cross-link on either side of the restriction site). These data also support a mixture of interstrand DNA cross-links in the major shifted dPAGE band resulting from reactions of these dirhodium compounds with the 123 bp DNA duplex.

The Dirhodium Adduct Profile on dsDNA Likely Includes Additional Covalent Linking Modes. Although the dPAGE data in this study show that all three dirhodium compounds bind to dsDNA and form interstrand cross-links with the duplex, the amount of cross-linked duplex in these gels does not account for all of the dirhodium modifications observed under the same reaction conditions in the DNA-binding curve data. For example, in the DNA-binding curve of Rh3 at an R_f of 0.002 (Figure 2), 80% of the dirhodium compound is bound to dsDNA after only 10 h of reaction. This corresponds to an R_b of ~0.0016 or ~0.2 dirhodium adducts per 123 bp (20% of a 123 bp duplex should be covalently modified with rhodium). Only 4% of the 123 bp DNA contains an interstrand cross-link by Rh3, however, as observed in lane 8 of Figure 3, after 23 h of reaction with a slightly higher initial Rh3 concentration ($R_f = 0.005$). The combination of these data suggests that, in addition to interstrand cross-links, Rh3 (as well as Rh1 and Rh2) forms other covalent adducts on dsDNA, possibly including monofunctional, intrastrand, and less stable interstrand adducts. Exploring these possibilities will be the focus of future studies.

CONCLUSIONS

In contrast to earlier claims, the present data indicate that dirhodium compounds bind covalently to dsDNA in aqueous buffer at neutral pH by forming interstrand cross-links and a variety of other adducts (monofunctional and intrastrand adducts). The reversal behavior of the interstrand cross-links under different conditions implies the presence of various coordination modes involving *ax*/*ax*, *ax*/*eq*, and *eq*/*eq* DNA interactions with the dirhodium core. These results reveal that potential mechanisms of biological action of dirhodium(II,II) carboxylate compounds should include inhibition of normal DNA processing by stable covalent Rh−DNA adducts. Further studies are in progress to characterize the adduct profile of dirhodium core binding in both interstrand and intrastrand dsDNA cross-links.

ACKNOWLEDGMENT

Prof. Nancy Gordon at the University of Southern Maine is gratefully acknowledged for use of and assistance with the GFAAS. K.R.D. thanks Johnson-Matthey for a generous gift of rhodium(III) trichloride.

SUPPORTING INFORMATION AVAILABLE

Sequence of the 123 bp DNA duplex (Figure S1), high-resolution dPAGE of Rh−123 bp DNA interstrand cross-links and an unmodified 278 bp duplex (Figure S2), dPAGE of *trans*-DDP adducts with a 123 bp duplex (Figure S3), and dPAGE of isolated Rh−123 bp DNA interstrand cross-links after heating in urea for various times (Figure S4). This material is available free of charge via the Internet at http://pubs.acs.org.

REFERENCES

1. Jamieson, E. R., and Lippard, S. J. (1999) Structure, recognition, and processing of cisplatin-DNA adducts, *Chem. Rev. 99*, 2467−2498.
2. Cohen, S. M., and Lippard, S. J. (2001) Cisplatin: from DNA damage to cancer chemotherapy, *Prog. Nucleic Acid Res. Mol. Biol. 67*, 93−130.
3. Reedijk, J. (2003) New clues for platinum antitumor chemistry: kinetically controlled metal binding to DNA, *Proc. Natl. Acad. Sci. U.S.A. 100*, 3611−3616.
4. Huang, J.-C., Zamble, D. B., Reardon, J. T., Lippard, S. J., and Sancar, A. (1994) HMG-domain proteins specifically inhibit the repair of the major DNA adduct of the anticancer drug cisplatin by human excision nuclease, *Proc. Natl. Acad. Sci. U.S.A. 91*, 10394−10398.
5. Zhai, X., Beckmann, H., Jantzen, H.-M., and Essigmann, J. M. (1998) Cisplatin-DNA adducts inhibit ribosomal RNA synthesis by hijacking the transcription human upstream binding factor, *Biochemistry 37*, 16307−16315.
6. Ohndorf, U.-M., Rould, M. A., He, Q., Pabo, C. O., and Lippard, S. J. (1999) Basis for recognition of cisplatin-modified DNA by high-mobility group proteins, *Nature 399*, 708−712.
7. Lee, K.-B., Wang, D., Lippard, S. J., and Sharp, P. A. (2002) Transcription-coupled and DNA damage-dependent ubiquitination of RNA polymerase II *in vitro*, *Proc. Natl. Acad. Sci. U.S.A. 99*, 4239−4244.
8. Millard, J. T., Weidner, M. F., Kirchner, J. J., Ribeiro, S., and Hopkins, P. B. (1991) Sequence preferences of DNA interstrand crosslinking agents: quantitation of interstrand crosslink locations in DNA duplex fragments containing multiple crosslinkable sites, *Nucleic Acids Res. 19*, 1885−1891.
9. Brabec, V. (2002) DNA modifications by antitumor platinum and ruthenium compounds: their recognition and repair, *Prog. Nucleic Acid Res. Mol. Biol. 71*, 1−68.
10. Farrell, N. (2004) Polynuclear Platinum Drugs, in *Metal Ions in Biological Systems* (Sigel, A., and Sigel, H., Eds.) Vol. 42, pp 251−296, Marcel Dekker, New York.
11. Farrell, N., Qu, Y., Feng, L., and Van Houten, B. (1990) Comparison of chemical reactivity, cytotoxicity, interstrand cross-linking and DNA sequence specificity of bis(platinum) complexes containing monodentate or bidentate coordination spheres with monomeric analogues, *Biochemistry 29*, 9522−9531.
12. Brabec, V., Kasparkova, J., Vrana, O., Cox, J. W., Qu, Y., and Farrell, N. (1999) DNA modifications by a novel bifuncional trinuclear platinum phase I anticancer agent, *Biochemistry 38*, 6781−6790.

13. Zhang, C. X., and Lippard, S. J. (2003) New metal complexes as potential therapeutics, *Curr. Opin. Chem. Biol. 7*, 481−489.
14. Chifotides, H. T., and Dunbar, K. R. (2005) Dirhodium Compounds, in *Multiple Bonds Between Atoms* (Cotton, F. A., Murillo, C. A., and Walton, R. A., Eds.) 3rd ed., Springer-Verlag, New York (in press).
15. Hughes, R. G., Bear, J. L., and Kimball, A. P. (1972) Synergistic effect of rhodium acetate and arabinosylcytosine on L1210, *Proc. Am. Assoc. Cancer Res. 13*, 120−120.
16. Howard, R. A., Kimball, A. P., and Bear, J. L. (1979) Mechanism of action of tetra-μ-carboxylatodirhodium(II) in L1210 tumor suspension culture, *Cancer Res. 39*, 2568−2573.
17. Erck, A., Rainen, L., Whileyman, J., Chang, I. M., Kimball, A. P., and Bear, J. L. (1974) Studies of rhodium(II) carboxylates as potential antitumor agents, *Proc. Soc. Exp. Biol. Med. 145*, 1278−1283.
18. Bear, J. L., Gray, H. B., Jr., Rainen, L., Chang, I. M., Howard, R., Serio, G., and Kimball, A. P. (1975) Interaction of rhodium-(II) carboxylates with molecules of biologic importance, *Cancer Chemother. Rep. 59*, 611−620.
19. Chang, I., and Woo, W. S. (1976) Effects of $Rh_2(O_2CC_2H_5)_4L_2$ on the replication of Ehrlich tumor cells *in vivo*, *Korean Biochem. J. 9*, 175−180.
20. Howard, R. A., Sherwood, E., Erck, A., Kimball, A. P., and Bear, J. L. (1977) Hydrophobicity of several rhodium(II) carboxylates correlated with their biologic activity, *J. Med. Chem. 20*, 943−946.
21. Zyngier, S., Kimura, E., and Najjar, R. (1989) Antitumor effects of rhodium(II) citrate in mice bearing Ehrlich tumors, *Braz. J. Med. Biol. Res. 22*, 397−401.
22. Reibscheid, E. M., Zyngier, S., Maria, D. A., Mistrone, R. J., Sinisterra, R. D., Couto, L. G., and Najjar, R. (1994) Antitumor effects of rhodium(II) complexes on mice bearing Ehrlich tumors, *Braz. J. Med. Biol. Res. 27*, 91−94.
23. Nothenberg, M. S., Zyngier, S. B., Giesbrecht, A. M., Gambardella, M. T. P., Santos, R. H. A., Kimura, E., and Najjar, R. (1994) Biological activity and crystallographic study of a rhodium propionate-metronidazole adduct, *J. Braz. Chem. Soc. 5*, 23−29.
24. Bear, J. L. (1986) Rhodium Compounds for Antitumor Use, in *Precious Metals 1985: Proceedings of the Ninth International Precious Metals Institute Conference* (Zysk, E. D., and Bonucci, J. A., Eds.) pp 337−344, International Precious Metals, Allentown, PA.
25. Clarke, M. J., and Stubbs, M. (1996) Interactions of Metallopharmaceuticals with DNA, in *Metal Ions in Biological Systems* (Sigel, A., and Sigel, H., Eds.) Vol. 32, pp 727−780, Marcel Dekker, New York.
26. Sorasaenee, K., Fu, P. K.-L., Angeles-Boza, A. M., Dunbar, K. R., and Turro, C. (2003) Inhibition of transcription in vitro by anticancer active dirhodium(II) complexes, *Inorg. Chem. 42*, 1267−1271.
27. Chifotides, H. T., Fu, P. K.-L., Dunbar, K. R., and Turro, C. (2004) Effect of equatorial ligands of dirhodium(II,II) complexes on the efficiency and mechanism of transcription inhibition *in vitro*, *Inorg. Chem. 43*, 1175−1183.
28. Rao, P. N., Smith, M. L., Pathak, S., Howard, R. A., and Bear, J. L. (1980) Rhodium(II) butyrate: A potential anticancer drug with cell cycle phase-specific effects in HeLa cells, *J. Natl. Cancer Inst. 64*, 905−911.
29. Howard, R. A., Spring, T. G., and Bear, J. L. (1976) The interaction of rhodium(II) carboxylates with enzymes, *Cancer Res. 36*, 4402−4405.
30. Chen, J., and Kostic, N. M. (1988) Binuclear transition-metal complexes as new reagents for selective cross-linking of proteins. Coordination of cytochrome *c* to dirhodium(II)-μ-tetraacetate, *Inorg. Chem. 27*, 2682−2687.
31. Trynda, L., and Pruchnik, F. (1995) Interactions of tetra-μ-acetatodirhodium(II) with human serum albumin, *J. Inorg. Biochem. 58*, 69−77.
32. Espósito, B. P., de Oliveira, E., Zyngier, S. B., and Najjar, R. (2000) Effects of serum albumin in some biological properties of rhodium(II) complexes, *J. Braz. Chem. Soc. 11*, 447−452.
33. Espósito, B. P., and Najjar, R. (2002) Interactions of antitumoral platinum group metallodrugs with albumin, *Coord. Chem. Rev. 232*, 137−149.
34. Tselepi-Kalouli, E., and Katsaros, N. (1990) The interaction of Rh(II) and Rh(III) with DNA, *J. Inorg. Biochem. 40*, 95−102.
35. de Souza Gil, E., Serrano, S. H. P., Ferreira, E. I., and Kubota, L. T. (2002) Electrochemical evaluation of rhodium dimer-DNA interactions, *J. Pharm. Biomed. Anal. 29*, 579−584.
36. Rainen, L., Howard, R. A., Kimball, A. P., and Bear, J. L. (1975) Complexes of rhodium(II) carboxylates with adenosine 5′-mono-, 5′-di-, and 5′-triphosphates, *Inorg. Chem. 14*, 2752−2754.
37. Pneumatikakis, G., and Hadjiliadis, N. (1979) Interactions of tetrakis-μ-acetato-dirhodium(II) with adenine nucleosides and nucleotides, *J. Chem. Soc., Dalton Trans.*, 596−599.
38. Rubin, J. R., Haromy, T. P., and Sundaralingam, M. (1991) Structure of the anti-cancer drug complex tetrakis(μ-acetato)-bis-(1-methyladenosine)dirhodium(II) monohydrate, *Acta Crystallogr. C47*, 1712−1714.
39. Alberding, N., Farrell, N., and Crozier, E. D. (1985) Examination of rhodium carboxylate antitumor agents complexes with nucleosides by extended X-ray absorption fine structure spectroscopy, *J. Am. Chem. Soc. 107*, 384−388.
40. Farrell, N. (1980) Metal-purine complexes: factors affecting specific binding, *J. Chem. Soc., Chem. Commun.*, 1014−1016.
41. Farrell, N. (1981) Adenine and adenosine derivatives of rhodium acetate, *J. Inorg. Biochem. 14*, 261−265.
42. Rubin, J. R., and Sundaralingam, M. (1984) Crosslinking of tRNAs by the carcinostatic agent dirhodium tetraacetate, *J. Biomol. Struct. Dyn. 2*, 525−530.
43. Dunbar, K. R., Matonic, J. H., Saharan, V. P., Crawford, C. A., and Christou, G. (1994) Structural evidence for a new metal-binding mode for guanine bases: implications for the binding of dinuclear antitumor agents to DNA, *J. Am. Chem. Soc. 116*, 2201−2202.
44. Crawford, C. A., Day, E. F., Saharan, V. P., Folting, K., Huffman, J. C., Dunbar, K. R., and Christou, G. (1996) *N7,O6* bridging 9-ethylguanine (9-EtGH) groups in dinuclear metal−metal bonded complexes with bond orders of one, two or four, *Chem. Commun.*, 1113−1114.
45. Chifotides, H. T., Koshlap, K. M., Pérez, L. M., and Dunbar, K. R. (2003) Unprecendented head-to-head conformers of d(GpG) bound to the antitumor active compound tetrakis(μ-carboxylato)-dirhodium(II,II), *J. Am. Chem. Soc. 125*, 10703−10713.
46. Chifotides, H. T., Koshlap, K. M., Pérez, L. M., and Dunbar, K. R. (2003) Novel binding interactions of the DNA fragment d(pGpG) cross-linked by the antitumor active compound tetrakis-(μ-carboxylato)dirhodium(II,II), *J. Am. Chem. Soc. 125*, 10714−10724.
47. Asara, J. M., Hess, J. S., Lozada, E., Dunbar, K. R., and Allison, J. (2000) Evidence for binding of dirhodium bis-acetate units to adjacent GG and AA sites on single-stranded DNA, *J. Am. Chem. Soc. 122*, 8−13.
48. Chifotides, H. T., Koomen, J. M., Kang, M., Dunbar, K. R., Tichy, S., and Russell, D. (2004) Binding of DNA purine sites to dirhodium compounds probed by mass spectrometry, *Inorg. Chem. 43*, 6177−6187.
49. Rempel, G. A., Legzdins, P., Smith, H., and Wilkinson, G. (1972) Tetrakis(acetato)dirhodium(II) and similar carboxylato compounds, *Inorg. Synth. 13*, 90−91.
50. Pimblett, G., Garner, C. D., and Clegg, W. J. (1986) Synthesis, crystal structure and spectroscopic properties of $[Mo(O_2CCH_3)_2(CH_3CN)_6](BF_4)_2$, $[Rh_2(O_2CCH_3)_2(CH_3CN)_6](BF_4)_2$ and $[Rh_2(O_2CCH_3)_2(CH_3CN)_4(py)_2](BF_4)_2$, *J. Chem. Soc., Dalton Trans.*, 1257−1263.
51. Cotton, F. A., and Felthouse, T. R. (1980) Ambidentate character of dimethyl sulfoxide in adducts of tetrakis(propionato)- and tetrakis(trifluoroacetato)dirhodium(II), *Inorg. Chem. 19*, 2347−2351.
52. Telser, J., and Drago, R. S. (1984) Action of strong acids on $M_2(O_2CR)_4$ species, *Inorg. Chem. 23*, 1798−1803.
53. Gallagher, S. R. (1994) Quantitation of DNA and RNA with absorption and fluorescence spectroscopy, in *Current Protocols in Molecular Biology* (Chanda, V. B., Ed.) John Wiley & Sons, New York.
54. Hartley, J. L., and Gregori, T. J. (1981) Cloning multiple copies of a DNA segment, *Gene 13*, 347−353.
55. Kane, S. A., and Lippard, S. J. (1996) Photoreactivity of platinum-(II) in cisplatin-modified DNA affords specific cross-links to HMG domain proteins, *Biochemistry 35*, 2180−2188.
56. Sambrook, J., Fritsch, E. F., and Maniatis, T. (1989) in *Molecular Cloning: A Laboratory Manual* (Ford, N., Nolan, C., and Ferguson, M., Eds.) 2nd ed., Cold Spring Harbor Laboratory Press, Plainview, NY.

57. Luce, R. A., and Hopkins, P. B. (2001) Chemical cross-linking of drugs to DNA, *Methods Enzymol. 340*, 396−412.
58. Brabec, V., and Leng, M. (1993) DNA Interstrand cross-links of *trans*-diamminedichloroplatinum(II) are preferentially formed between guanine and complementary cytosine residues, *Proc. Natl. Acad. Sci. U.S.A. 90*, 5345−5349.
59. Erck, A., Sherwood, E., Bear, J. L., and Kimball, A. P. (1976) The metabolism of rhodium(II) acetate in tumor-bearing mice, *Cancer Res. 36*, 2204−2209.
60. Chifotides, H. T., Hess, J. S., Angeles-Boza, A. M., Galán-Mascarós, J. R., Sorasaenee, K., and Dunbar, K. R. (2003) Structural evidence for monodentate binding of guanine to the dirhodium(II,II) core in a manner akin to that of cisplatin, *Dalton Trans.*, 4426−4430.
61. Perlepes, S. P., Huffman, J. C., Matonic, J. H., Dunbar, K. R., and Christou, G. (1991) Binding of 2,2′-bipyrine to the dirhodium-(II) tetraacetate core: unusual structural features and biological relevance of the product $Rh_2(OAc)_4(bpy)$, *J. Am. Chem. Soc. 113*, 2770−2771.
62. Lide, D. R. (2000−2001) *CRC Handbook of Chemistry and Physics*, 81st ed., CRC Press, New York.
63. Hopkins, P. B., Millard, J. T., Woo, J., Weidner, M. F., Kirchner, J. J., Sigurdsson, S. T., and Raucher, S. (1991) Sequence preferences of DNA interstrand cross-linking agents: importance of minimal DNA structural reorganization in the cross-linking reactions of mechlorethamine, cisplatin and mitomycin C, *Tetrahedron 47*, 2475−2489.
64. Shafranskii, V. N., and. Mal'kova, T. A. (1975) Compounds of dirhodium(II) diaquatetraacetate with urea and its derivatives, *J. Gen. Chem. USSR 45*, 1051−1054.
65. Pittet, P.-A., Dadci, L., Zbinden, P., Abou-Hamdan, A., and Merbach, A. E. (1993) High-pressure proton NMR study of acetonitrile exchange kinetics on $[Rh_2(CH_3CN)_{10}]^{4+}$ and ^{17}O NMR investigation of aqueous solutions of $[Rh_2(H_2O)_{10}]^{4+}$, *Inorg. Chim. Acta 206*, 135−140.
66. Ahmad, S., Isab, A. A., and Ahmad, S. (2003) ^{1}H, ^{13}C, ^{15}N NMR and IR spectroscopic studies of a Rh(II) complex of thiourea, *J. Coord. Chem. 56*, 1587−1595.
67. Sorasaenee, K., Galán-Mascarós, J. R., and Dunbar, K. R. (2002) Reactivity studies of anticancer active dirhodium complexes with 2-aminothiophenol, *Inorg. Chem. 41*, 433−436.
68. Sorasaenee, K., Galán-Mascarós, J. R., and Dunbar, K. R. (2003) Isolation of the novel dirhodium(II/II) thiolate compound $Rh_2(\eta^1\text{-}C_6H_6S)_2(\mu\text{-}C_6H_5S)_2(bpy)_2$, *Inorg. Chem. 42*, 661−663.

BI0486637